Fabrication and high temperature characteristics of microtapered long period fiber gratings based on microfibers

BINGCHUAN WANG[1], LIYONG REN[2], XUDONG KONG[3], YIPING XU[1,*], KAILI REN[3], WENXING YANG[1], SHUBO CHENG[1], YUHUI LI[1], JIABAO JIANG[1]

[1]*School of Physics and Optoelectronic Engineering, Yangtze University, Jingzhou 434023, China*

[2]*School of Physics & Information Technology, Shaanxi Normal University, Xi'an 710119, China*

[3]*State Key Laboratory of Transient Optics and Photonics, Xi'an Institute of Optics and Precision Mechanics, Chinese Academy of Sciences, Xi'an 710119, China*

Based on the photoelastic effect, a new technology is used to fabricate high quality microtapered long period fiber gratings (MLPFGs) from microfibers. The effects of different periods and number of tapers on the grating spectrum have been explored. The high temperature characteristics of the grating were studied. The results show that MLPFG fabricated from a microfiber has good high temperature stability. With the increase of temperature, the spectrum of grating with a period of 685 μm has the same change trend as that of grating with a period of 670 μm. The temperature sensing sensitivities of gratings with periods of 685 μm and 670 μm are 0.0203 nm°C^{-1} and 0.01741 nm°C^{-1}, respectively. The critical temperature at which the spectrum of the fabricated MLPFG changes irreversibly is between 600°C and 800°C, which is more than 100°C higher than that reported previously. Another advantage of this type of grating is that it can be used to make torsion sensor. The measurement range is larger than that of grating directly tapered from a single mode fiber (SMF). By observing the shifts of resonant wavelengths, the torsion angle can be determined without taking other measures.

(Received June 3, 2021; accepted December 6, 2022)

Keywords: Long period fiber grating, Microfiber, Optical fiber optics, High temperature characteristics, Torsion sensing

1. Introduction

Long period fiber gratings (LPFGs) possess periodic perturbation of the refractive index distribution, with the period order of 100 μm to 1 mm [1]. LPFGs can be written in different kinds of fibers, such as photonic crystal fiber [2] and polarization-maintaining panda fiber [3,4]. Due to the low cost of fabrication and high compatibility with common communication system, standard single mode fibers (SMFs) are most widely used to write LPFGs. In recent years, LPFGs inscribed in the microfibers have been attracting significant attentions. Because the microfibers tapered from SMFs possess tiny diameter, which can miniaturize the optical components and be also easily compatible with other system. Different methods have been explored in recent years to inscribe LPFGs in microfibers, such as periodically modifying the surface of the microfibers by including femtosecond IR laser [5], periodically dipping Teflon droplet along thinned fibers [6], and helically coiling one thinned fiber onto another [7,8]. Besides the above efforts, periodically tapering the microfibers to fabricate the microtapered long period fiber gratings (MLPFGs) have been widely investigated, because this method is simple and feasible. One of the key steps for fabricating this kind of MLPFGs is to soften the microfibers. Yoon et al. employed oxyhydrogen flame as the heating source to soften the microfibers [9]. Unfortunately, the softened region with oxyhydrogen flame is too big to achieve MLPFGs with small period. In addition, the oxyhydrogen flame is not stable, which results in the inconsistent fabrication process of MLPFGs. Fan et al. employed arc discharging in a commercial splicer as the heating source to soften the microfibers [10]. However, the arc discharging may contaminate the surface of MLPFGs, resulting in degrading the quality of the fabricated MLPFGs. Xuan et al. employed CO_2 lasers as the heating source because of the strong light absorption at the wavelength of 10.6 μm [11]. However, only one laser beam is focused on the microfiber, which causes that the transverse section of the microfiber cannot be heated uniformly and softened, resulting in degenerating the quality of the fabricated MLPFGs.

In this paper, we used a different technique which not only avoids those disadvantages mentioned previously, but also has its own advantages to fabricate MLPFGs based on microfibers and investigated the influence of fabrication parameters on the spectrum. The main fabrication mechanism of this kind of grating is physical deformation [12]. Such physical deformation induces the change of effective refractive index in the microfiber. This kind of gratings are every suitable for extreme situation. So, investigating the spectral characteristics in extreme situation is desired and important. High temperature is one kind of extreme situation. Exploring the high temperature characteristics of MLPFGs based on microfibers is necessary. But so far, there has not been relevant report about this. Therefore, we studied, for the first time to our knowledge, the high temperature characteristics of MLPFGs based on microfibers, which can provide reference for other research and application of this kind of gratings. In addition, the torsion sensing of this grating was also explored.

2. Fabrication technique of MLPFGs based on microfibers

For fabricating this type of grating, we used a technique similar to that described in [13-15] but with some modification. The improvement is that the SMF with a diameter of 125 μm was first drawn into a microfiber with a waist cone diameter of 30 μm. Because the fabrication process of this grating is easy to control and this grating has an ideal spectrum. (Reference 9 has studied the influence of the waist diameter on transmission characteristics). The diameter of the microfiber is basically uniform, and its length can accommodate more than ten periods. The optical fiber was drawn into microfiber by heating in a micro furnace. In the process of fabricating microfiber, one end of the grating is pushed by a motor, and the other end is pulled by another motor. The diameter of the microfiber is controlled by controlling the velocity ratio of the two motors. Suppose the diameter of the microfiber is r, the diameter of the optical fiber is R, the speed of the push motor is v_1 and the speed of the pull motor is v_2, then the diameter of the microfiber r can be obtained by the formula $(r/R)^2= v_1/ v_2$. The light path diagram of the heating source and the structure diagram of this fusion splicer are shown in Fig. 1(a) and (b), respectively. The fabrication process is roughly as follows：Firstly, fix the microfiber that has been fabricated between two rotation motors. Secondly, let the two translation motors move in the same direction with a constant speed V. Thirdly, by controlling the stop time of two translation motors, the motor in the back stops first and the motor in front stops later. The move time of the motor in the front is T_f . In this way, there will be a certain stress in the axial direction of the fiber. Fourthly, heat and soften the fiber by the laser source releasing CO_2 laser. Because of the axial stress in the fiber, the fiber at the melting point can be easily drawn into two symmetrical cones. The period P of the grating is equal to the motion distance of the translation motor in the front. Fifthly, repeat the above four operations. In order to observe the transmission spectrum in real time, we set up the system shown in Fig. 2.

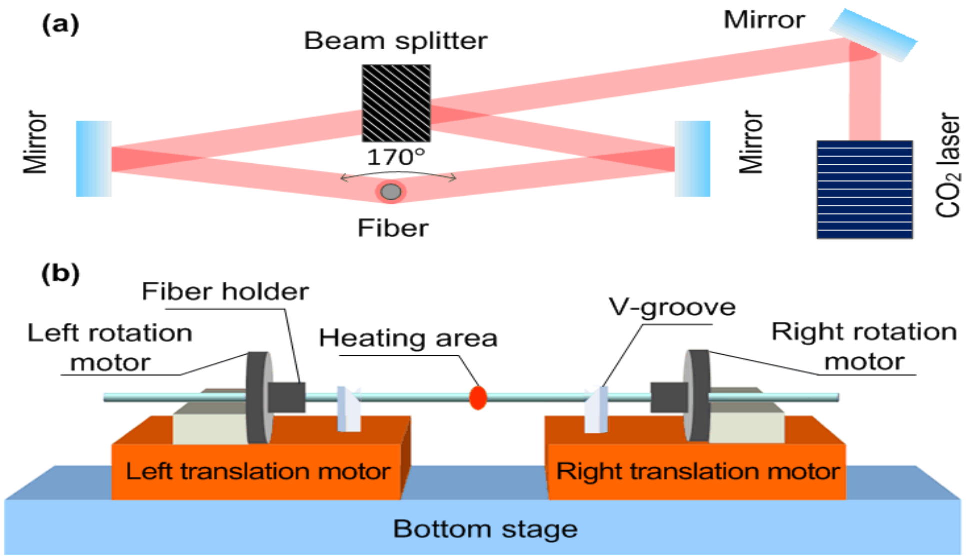

Fig. 1. (a) Optical path diagram of CO_2 fusion splicer; (b) Overall diagram of CO_2 fusion splicer (color online)

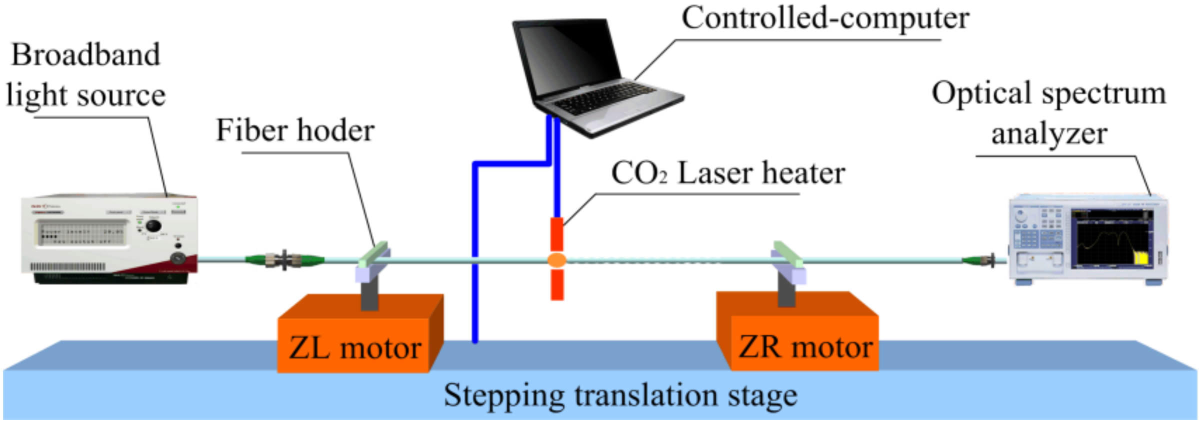

Fig. 2. Systematic diagram of fabricating MLPFGs based on microfibers (color online)

The fabrication is under control by writing a fully program we designed in the controlled computer. In the program, we can change laser power, exposure time, the motion time of two translation motors, the number of tapers and so on. In this paper, gratings with different parameters are fabricated by changing the motion time of two translation motors and the number of tapers, other controllable parameters remain unchanged.

This technique has the following five advantages [15]: First, a fusion splicer (Fujikura, LZM-100) which has low maintenance cost and long-term consistency is adopted. Second, the CO_2 laser in this fusion splicer utilizes special closed-loop power stabilization techniques, resulting in power fluctuation within 0.5%, which can achieve a highly repeatable and smooth heating process. Third, the heating length (0.3 mm) of this fiber is much smaller than that heating length (0.5 mm) using a sapphire tube heated by the laser as a miniature oven with a constant temperature inside. Fourth, compared with the arc discharge method, our method is cleaner and pollutes the grating less. Fifth, compared with the method which uses a single CO_2 laser beam to heat and soften the fiber, this method softens the fiber more evenly and produces gratings with higher quality.

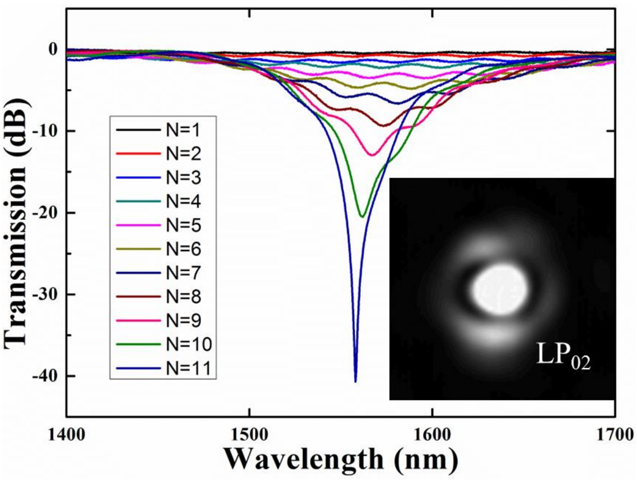

Fig. 3. Transmission spectra of the grating with a period of 660 μm under the conditions of different number of tapering. Inset is the near-field mode field distribution of grating with an N = 40 at the wavelength of 1558 nm (color online)

Fig. 3 and Fig. 4 show the influences of fabrication parameters on spectra of MLPFGs based on microfibers. When we fabricated a grating with a period of 660 μm, the spectra corresponding to different N (N is the number of tapers) were recorded, as shown in Fig. 3. It can be seen from this figure that the transmission loss is about 0.5 dB, the resonant dip depth can reach -40 dB. This shows that high quality gratings can be produced by this technology. From the change of the spectra, it can be found that the dip depth increases as the number of tapers increases. When the number of tapers reaches 11, the dip depth reaches a maximum value. Under the same fabrication parameters, we fabricated a grating with an N = 11. Insert in Fig. 3 exhibits a Charge-coupled Device (CCD) image of the field distribution of the cladding mode coupled from the core mode passing through the fabricated MLPFG at the resonant wavelength of 1558 nm, which corresponds to the coupled cladding mode of LP02. In addition, as the number of tapers increases, the full width at half maximum (FWHM) of the resonant dip decreases gradually. These two changing trends of spectra are consistent with those mentioned in [15]. While the resonant dip drifts to the shortwave direction as the number of tapers increases, which opposites to that in [15].

In order to explore the effect of grating period on grating spectrum, we have also fabricated gratings with different periods. The grating spectra were recorded when their dip depth reached the maximum. For comparison purposes, they were drawn in the same picture, as shown in Fig. 4. As can be seen from the figure, with the increase of grating period, the resonant dip drifts to the shortwave direction, while the FWHM and the dip depth almost unchanged. Taking advantage of this feature, gratings can be made into filters adapted to different needs [16-19].

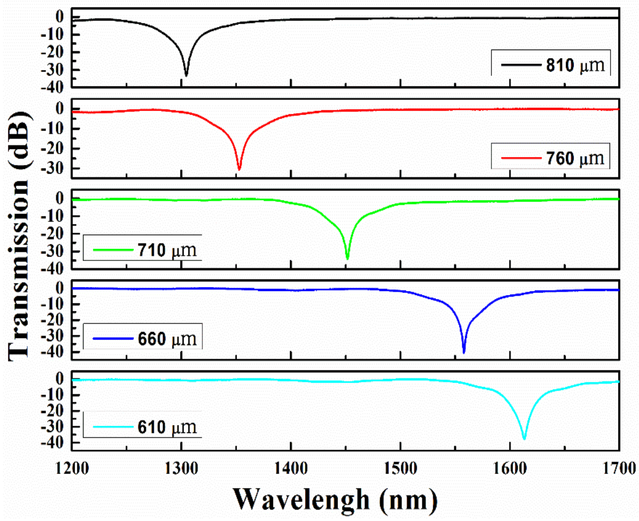

Fig.4. Spectra of gratings with periods of 610 μm, 660 μm, 710 μm,760 μm and 810 μm (color online)

3. High temperature characteristics of the fabricated MLPFGs based on microfibers

For exploring the high temperature characteristics of this type of grating, the fabricated grating was placed in a Molybdenum-wound furnace and was maintained with no traction or strain. The temperature of the Molybdenum-wound furnace can be adjusted and the maximum temperature can reach 1700°C.

3.1. Wavelength shift at high temperature

We have investigated the thermal behavior of gratings with periods of 685 μm and 670 μm. Their transmission spectra were recorded after the temperature has stabilized for ten minutes. Fig. 5 shows the variation of resonant wavelengths with the temperature.

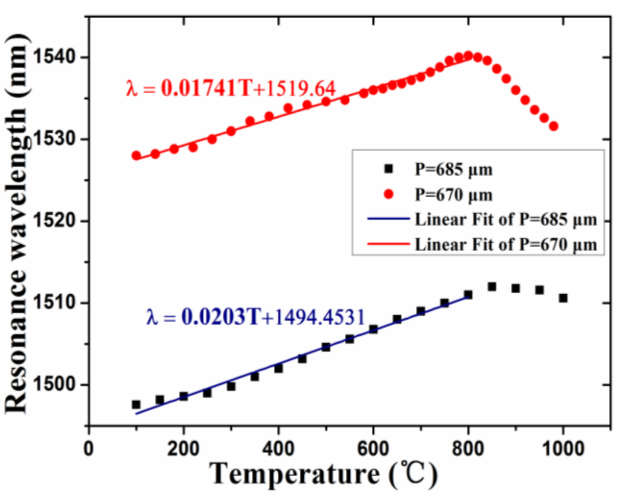

Fig. 5. Resonant wavelengths of the gratings with periods of 685 μm and 670 μm as a function of temperature (color online)

We can see that before the temperature rises to 850°C, both gratings show the similar behavior that the resonant dips drift almost linearly toward the long wave direction as the temperature increases. This phenomenon is the same as the prediction in the previous references [20-22]. In this temperature range, the sensitivities of gratings with periods of 685 μm and 670 μm are 0.0203 nm°C^{-1} and 0.01741 nm°C^{-1}, respectively. It is estimated that this shift is mainly determined by the temperature dependence of the refractive index [17,18]: $\delta\lambda/\delta T \sim \Lambda(n_c\text{-}n_{cl})\delta n_{cl}/\delta T$, where n_c and n_{cl} are the refractive indexes of the core and the cladding, respectively, $\delta n_{cl}/\delta T$ is taken for silica glass[23]. The shift due to the grating period change ($\delta\lambda/\delta T = \lambda\alpha$, where α is the thermal expansion coefficient, for silica $\alpha < 10^{-6}$) is an order of magnitude smaller. However, at high temperatures, due to a much stronger dependence on temperature [19], the role of the thermal expansion coefficient becomes as important as that of the refractive index [21].

When the temperature exceeds 850°C, we can see from Fig. 5 that the resonant dips drift to the short wave direction as the temperature increases. It proves that, when it exceeds a certain range, temperature is no longer the decisive factor in drift. This behavior may be the result of relaxation of the fiber residual stress and rearrangement of the glass structure [20,21].

3.2. Annealing of the gratings

To better understand the thermal behavior of this type of gratings, we conducted an annealing experiment. In the experiment, two gratings with the same parameters (N is 11 and period is 685 μm) were heated to 400°C and 600°C respectively, and then cooled to normal temperature (20°C) for one hour. The spectra of these two gratings after annealing were recorded and compared with that spectrum of the grating with the same parameters fabricated at normal temperature, as shown in Fig. 6. No degradation and shift of the spectrum were observed. This high thermal stability is an important advantage compared with UV-induced gratings [24] and electric-arc-induced gratings [25]. Table 1 shows the temperatures at which the spectra of different kinds of gratings change irreversibly. It can be seen from this Table that the critical temperature of our fabricated MLPFGs based on microfibers is over 100°C higher than that of other two kinds of gratings.

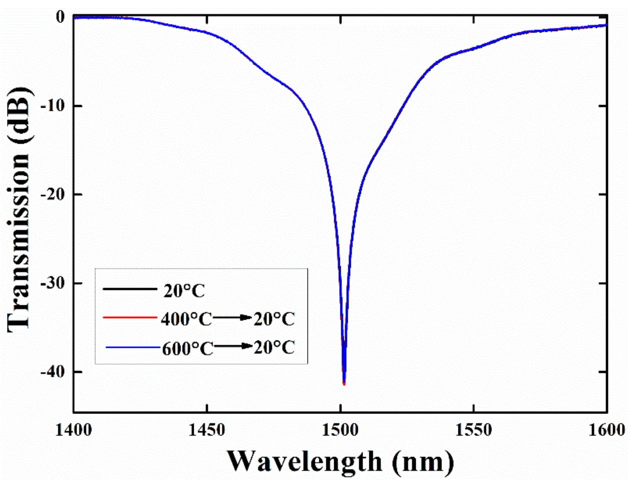

Fig. 6. Spectra of gratings with a period of 685 μm measured after annealing from 400 ℃ and 600 ℃ to 20 ℃ (color online)

In order to investigate the temperature effect at higher temperature, we have performed annealing at

800°C and 1000°C. Fig. 7 shows the spectral comparison of grating fabricated at normal temperature (20°C) and gratings cooled to normal temperature for one hour from 800°C and 1000°C, respectively. From Fig. 7 we can see that they exhibit a serious degradation (from 10 dB to 20 dB) and an irreversible shift that the resonant dips drift to the short wave direction. The drift direction is consistent with that of resonant dips when the temperature exceeds 850°C in Fig. 5. This phenomenon is also reported for pulsed CO_2 laser-induced LPFGs [26]. It may be due to the relaxation of the fiber residual stress and to the rearrangement of the glass structure [20,21].

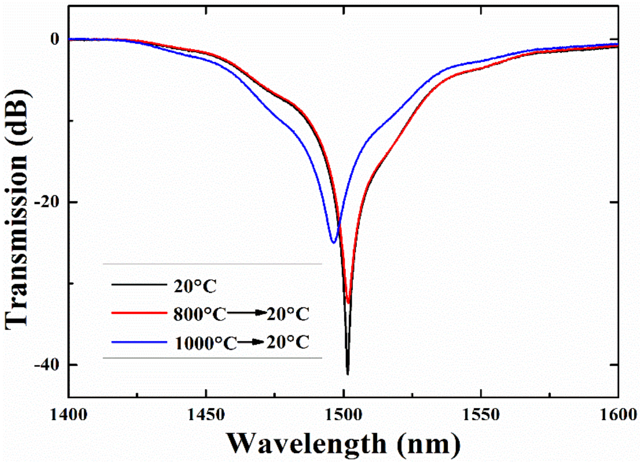

Fig. 7. Spectra of a grating with a period of 685 μm measured after annealing from 800 ℃ and 1000 ℃ to 20 ℃ (color online)

Table 1. The critical temperatures at which an irreversible change in the spectrum occurs

Types of Gratings	The critical temperatures at which the spectrum changes irreversibly
UV-induced gratings (Dianov et al.) [24]	400℃
Electric-arc-induced gratings (Godbout et al.) [25]	500℃
MLPFGs based on microfibers (ours)	600℃~800℃

4. Sensing of torsion

In addition to good high temperature stability, physical deformation also has a good performance in torsion sensing. The torsion sensing characteristics of grating which was fabricated by directly tapering SMF have been explored in [15]. In this paper, we explored the torsion sensing characteristics of MLPFGs based on microfibers at room temperature of 20°C. In this experiment, a grating with an N of 11 and a period of 685 μm was fixed between two rotation motors with a distance of 80 mm. Twisting the grating by rotating one of the two rotation motors from 0° to 2520° in steps of 360°. The resonant wavelengths λ corresponding to different mechanical torsion rate α_M (α_M is equal to the ratio of the torsion angle to the distance between two rotation motors.) were plotted in Fig. 8.

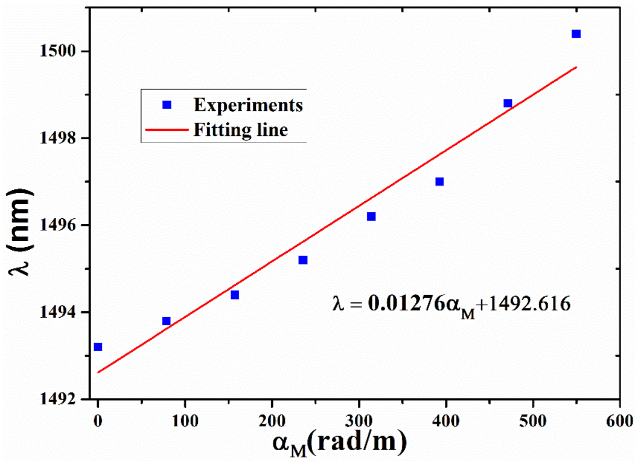

Fig. 8. Resonant wavelengths of grating as a function of the mechanical torsion rate α_M

From Fig. 8 we can see that the wavelengths of the resonant dips drift toward the long wave direction as the torsion rate α_M increases. According to the experimental data, the sensitivity of the grating is calculated to be about 0.01276 nm·m·rad^{-1}. And the measurement range of this grating is 0 - 550 rad/m, which is larger than that of the grating fabricated by directly tapering SMF [15]. But this grating can't judge the torsion direction. Because torsion changes the stress of the grating, but the structure of the grating is along the axial direction, and there is almost no angular refractive index modulation, so it is impossible to judge the torsion direction. MLPFG based on SMF can judge the torsion direction because the diameter of the fiber is bigger. In the process of grating fabrication, the cross-section of the fiber is heated unevenly, which leads to the inhomogeneous modulation of the refractive index, that is to say, there is a change of the refractive index along the radial direction. However, when the fiber diameter is small, the change of radial refractive index can be ignored.

5. Conclusion

MLPFGs based on microfibers were fabricated successfully by using a fusion splicer. The fabrication process of this grating with high repeatability is simple and stable. Both number of tapers and period can influence the grating spectra. Gratings meeting different requirements can be obtained by changing the number of tapers and the period. In the experiment of exploring the high temperature characteristics, before the temperature rises to 850°C, the resonant dips drift toward the long wave direction as the temperature increases, the sensitivity is about 0.02 nm°C^{-1}. The temperature at which the spectrum changes irreversibly is greater than 600°C. These characteristics can be used to make thermal sensors suitable for high temperature environment. In terms of torsion sensing characteristics, the sensitivity is 0.01276 nm·m·rad^{-1}. Without other measurements, the angle of torsion can be judged by observing the spectrum, and the measurement range is larger than that grating which is directly tapered on SMF.

Acknowledgements

This work was supported in part by the National Natural Science Foundation of China (NSFC) (61605018, 11904032), the Natural Science Foundation of Shaanxi Province (2021JM-204), the Hubei Natural Science Foundation of China (2016CFC767), the Doctoral Scientifific Research Startup Foundation of Yangtze University (801080010128), the Open Research Fund of State Key Laboratory of Transient Optics and Photonics (SKLST201612).

References

[1] J. R. Ranjan, F. Esposito, S. Campopiano, A. Iadicicco, SPIE Optical Sensors **10231**, 102312N (2017).
[2] F. Tian, J. Kanka, B. Zou, K.S. Chiang, H. Du, Optics Express **21**(11), 13208 (2013).
[3] A. Iadicicco, R. Ranjan, F. Esposito, S. Campopiano, IEEE Photonic Tech. L. **29**(18), 1533 (2017).
[4] R. Ranjan, F. Esposito, S. Campopiano, A. Iadicicco, IEEE Sens. J. **17**(21), 6953 (2017).
[5] H. F. Xuan, W. Jin, S. J. Liu, Optics Letters **35**(1), 85 (2010).
[6] X. Y. Zhang, Y. S. Yu, C. Chen, C. C. Zhu, R. Yang, Z. J. Liu, J. F. Liang, Q. D. Chen, H. B. Sun, IEEE Photonic Tech. L. **26**(24), 2503 (2014).
[7] L. P. Sun, J. Li, L. Jin, B. O. Guan, Optics Express **20**(16), 18079 (2012).
[8] F. Ren, D. W. Ge, J. H. Li, Z. B. Li, Y. Q. He, Z. Y. Chen, Opt. Commun. **360**, 15 (2016).
[9] M. S. Yoon, H. J. Kim, S. J. Kim, Y. G. Han, Optics Lett. **38**(15), 2669 (2013).
[10] P. Fan, L. P. Sun, Z. Yu, J. Li, C. Wu, B. O. Guan, Optics Express **24**(22), 25380 (2016).
[11] H. F. Xuan, W. Jin, M. Zhang, Optics Express **17**(24), 21882 (2009).
[12] C. D. Poole, J. P. Meester, H. M. Presby, Electron Lett. **30**(17), 1437 (2002).
[13] X. D. Kong, K. L. Ren, L. Y. Ren, J. Liang, H. J. Ju, Appl. Optics **56**(16), 4702 (2017).
[14] K. L. Ren, L. Y. Ren, J. Liang, X. D. Kong, H. J. Ju,

Z. X. Wu, IEEE Photonic Tech L. **29**(13), 1085 (2017).

[15] B. C. Wang, L. Y. Ren, X. D. Kong, Y. P. Xu, K. L. Ren, W. X. Yang, S. B. Cheng, F. Chen, F. Song, Optik **207**, 164445 (2020).

[16] A. M. Vengsarkar, P. J. Lemaire, J. B. Judkins, V. Bhatia, T. Erdogan, J. E. Sipe, J. Lightwave Technol. **14**(1), 58 (1996).

[17] O. Duhem, A. DaCosta, J. F. Henninot, M. Douay, Electron Lett. **35**(12), 1014 (1999).

[18] V. Bhatia, A. M. Vengsarkar, Opt Lett. **21**(9), 692 (1996).

[19] B. H. Lee, J. Nishii, Electron Lett. **34**(21), 2059 (1998).

[20] G. Humbert, A. Malki, J. Opt. A: Pure Appl. Op. **4**, 194 (2002).

[21] G. Rego, O. Okhotnikov, E. M. Dianov, M. Ketata, J. Lightwave Technol. **19**(10), 1574 (2002).

[22] G. Humbert, A. Malki, C. Prioleau, M. Ketata, Proc. SPIE **4417**, 427 (2001).

[23] R. Brückner, J. Non Cryst. Solids **5**(3), 177 (1970).

[24] E. M. Dianov, V. I. Karpov, A. S. Kurkov, M. V. Grekov, European Conference on Optical Communication ECOC, (2002).

[25] N. Godbout, X. Daxhelet, A. Maurier, S. Lacroix, 24th European Conference on Optical Communication, ECOC '98 (IEEE Cat. No.98TH8398), Madrid, Spain. 1, 397-398 (1998).

[26] D.D. Davis, T. K. E. N. Gaylord, Glytsis, S. C. Mettler, Electron Lett. **35**(9), 740 (2002).

*Corresponding author: ypxu@yangtzeu.edu.cn